Jahn-Teller coupling and fragmentation after core-shell excitation in CF_4 investigated by partial-ion-yield spectroscopy

Renaud Guillemin,[1,2] Wayne C. Stolte,[3] Maria Novella Piancastelli,[4] and Dennis W. Lindle[3]

[1]*Université Pierre et Marie Curie, Laboratoire de Chimie Physique-Matière et Rayonnement, UMR 7614, 11 rue Pierre et Marie Curie, FR-75231 Paris Cedex 05, France*

[2]*CNRS, Laboratoire de Chimie Physique-Matière et Rayonnement, UMR 7614, 11 rue Pierre et Marie Curie, FR-75231 Paris Cedex 05, France*

[3]*Department of Chemistry, University of Nevada, Las Vegas, Nevada 89154-4003, USA*

[4]*Department of Physics and Astronomy, Uppsala University, P.O. Box 516, SE-75120 Uppsala, Sweden*

(Received 19 August 2010; published 22 October 2010)

We investigate fragmentation processes induced by core-level photoexcitation in CF_4 at both the carbon and fluorine K edges by means of partial-ion-yield spectroscopy. The molecule CF_4 is a textbook example of systems in which Jahn-Teller coupling strongly manifests itself in the photoabsorption spectrum. Spectral features related to Jahn-Teller and quasi-Jahn-Teller splitting are observed, and important differences in the fragmentation pathways are revealed depending on the symmetries of the core-excited states. We interpret these experimental observations on the grounds of symmetry lowering from the T_d to the C_{3v} point group as well as preferential orientation with respect to the polarization vector of the incident radiation.

DOI: 10.1103/PhysRevA.82.043427 PACS number(s): 33.80.Gj, 33.80.Eh

I. INTRODUCTION

Tetrahedral species with the general formula CX_4 (X = H, F, Cl) have been extensively studied with x-ray photoabsorption, photoelectron spectroscopy, and related x-ray techniques. In particular, topics such as the relative intensities of transitions from core levels to antibonding molecular orbitals or Rydberg states, Jahn-Teller and quasi-Jahn-Teller coupling, and the dissociative nature of core-excited intermediate states and valence-ionized final states have been discussed in several papers (see, e.g., [1–8] for CH_4, [9–19] for CF_4, and [4,15] for CCl_4). A summary of the electronic properties of all three molecules is given in [20] together with high-resolution photoabsorption data.

One of the most interesting observations stemming from the comparison between CH_4 and CF_4 photoabsorption experiments performed around the C K edge is the relative intensity of below-threshold structures related to transitions to empty molecular orbitals versus Rydberg states: while the Rydberg series is dominant in methane, in tetrafluoromethane there are prominent broad structures at lower photon energy followed by a series of sharp peaks attributable to the Rydberg series. Such a striking difference in two structurally similar molecules has been attributed to a cagelike effect induced by the electronegative fluorine atoms, which creates a potential barrier that pushes the Rydberg states to a larger distance with respect to the antibonding orbitals. This generally accepted interpretation should be supported by a method which is able to distinguish between the Rydberg and antibonding character of the excited states.

Another topic of interest is the extent of Jahn-Teller and quasi-Jahn-Teller coupling in the series of molecules. The high symmetry of tetrahedral molecules implies that at the C K edge, the dipole-allowed transitions are from the C 1s level with a_1 symmetry to the empty molecular orbitals of t_2 symmetry. However, the threefold degeneracy of the excited state can be removed by Jahn-Teller splitting, and this reduction in symmetry can allow transitions to the nominally symmetry forbidden a_1 state. Therefore, in CF_4, the lowest-energy region of the absorption spectrum below threshold contains a broad structured band which has been ascribed to transitions to the t_2-Jahn-Teller-split states, plus quasi-Jahn-Teller coupling between the forbidden a_1 transition and the a_1 state resulting from the t_2-Jahn-Teller splitting.

Several groups have investigated the absorption spectrum of CF_4 at the carbon K edge [9–12]. Detailed calculations assigning the spectral features are reported in [13]. The CF_4 molecule has also been examined by electron energy loss spectroscopy (EELS) and near-edge x-ray-absorption fine structure (NEXAFS) spectroscopy at the fluorine K edge [4,16]. Threshold and photoion-photoion coincidence spectra have been studied as well [16]. Resonant-Auger decay has been reported in [11], and core-excitation-induced photofragmentation has been discussed in [18]. Photofragmentation around both the C and F K edges has been studied with time-of-flight mass spectrometry [19].

We report here a detailed study of the decay properties of core-excited and core-ionized CF_4 around both the C and F K edges. The study has been performed using partial-ion-yield spectroscopy, where a single mass-selected positive or negative ion is collected as a function of photon energy in an interval including one or more ionization thresholds. The underlying physics is the following: after creation of a molecular core hole by an incident photon, some of the valence electrons, which form the chemical bonds, are ejected via the dominant Auger process, after which the molecule usually dissociates into fragment ions and/or neutrals. In order to discuss photofragmentation processes in more detail, it is common to consider the regions below and above the ionization threshold separately. Below threshold, following excitation of a core electron to a bound but unoccupied molecular orbital, a core hole decays via resonant-Auger processes, either by participator or spectator decay [21,22]. After resonant-Auger decay, which typically produces singly ionized states, the molecule is often unstable and dissociates

into ionic or neutral fragments. Above the ionization threshold, normal Auger decay dominates, yielding doubly charged ions that are even more likely to dissociate. Compared to photoabsorption or absorptionlike measurements, such as total-electron or total-ion yield (including the NEXAFS for gas-phase and adsorbed species), there is an advantage in monitoring partial-ion channels that are more selective with respect to different types of resonances. Moreover, our experimental apparatus possesses the capability to detect either positively charged species (cations) or negatively charged species (anions). Partial-anion yields in particular are more selective than most other single-channel measurements. The possibility of observing single ion channels in the region of the Jahn-Teller-split states can shed light on the relative positions of such features, which being broad and overlapping cannot be separated in multichannel measurements, but are better resolved in our spectra due to subtle differences in fragmentation patterns. Such observations also can clarify spectral assignments in terms of the energy ordering of the resonances.

One interesting finding derived from previous partial-ion-yield measurements is that below threshold, the relative intensity of spectral features related to core-to-Rydberg excitation increases on a relative basis because the fragmentation process is more extensive. In other words, for smaller fragments, ion yields for Rydberg states are stronger than for larger fragments. This is directly related to spectator decay being more likely following excitation to diffuse Rydberg orbitals, with the result that many or most of the final two-hole–one-particle states are dissociative [23–25]. In the present case, such effects can be exploited to assess the nature of some of the spectral features below the C K edge as stemming from transitions to states with pure or almost-pure Rydberg character. We also observe enhanced production of doubly positively charged species and negatively charged fragments in the region of Rydberg transitions compared to transitions to molecular orbitals, again due to the instability of final states reached after decay of core-to-Rydberg excitations.

A peculiar characteristic of the CF_4 absorption spectra is that above both the C and F K edges, the cross section is quite low, and the ionization thresholds are not clearly visible. We confirm this finding with our partial-ion-yield results, and we attribute the absence of a clearly evident threshold in most of the yields to the fact that the fragmentation patterns do not change appreciably between the resonance states just below threshold as compared to those just above threshold in the continuum, due to excitation of states that have a strong propensity to dissociate. Finally, the possible existence of a shape resonance above threshold has been reported for CF_4 [9,26], but its intensity is very low in photoabsorption measurements. We confirm this characteristic in the partial-ion yields.

II. EXPERIMENTAL

Experiments were performed on beamline 8.0.1.3 at the Advanced Light Source, Lawrence Berkeley National Laboratory. This 5-cm-period undulator beamline is equipped with three interchangeable spherical gratings (150, 380, and 925 lines/mm) for high spectral resolution and high flux and provides 10^{11} to 6×10^{15} photons/s in the 80–1400 eV photon-energy range with a maximum resolving power of $E/\Delta E < 8000$. The monochromator calibration near the carbon and fluorine K edges was performed by comparison to high-resolution photoabsorption measurements [20]. Contamination by third-order light from the undulator passing through the monochromator accounts for less than 1% of the total photon flux.

Ion mass and charge characterization was obtained using a 180° magnetic mass analyzer with a resolution of approximately 1 amu in 65. The apparatus has been described in detail elsewhere [27]. Briefly, fragment ions are created by interaction with the light beam at the exit of an effusive-jet gas cell. Ions are extracted from the gas cell by an electric field and focused onto the entrance slit of the analyzer by an electrostatic lens. They are then deflected between the poles of the analyzer and refocused onto the exit slit before being detected by a channel electron multiplier (CEM). The potentials of the analyzer can be tuned and/or switched in polarity to select fragments with a specific mass and charge. A total cation yield was measured with a CEM located on the opposite side of the gas cell with respect to the spectrometer entrance slit. A circular aperture through the pusher plate allows all positive ions to be detected when the polarities are switched for anion measurements. The photon flux was recorded by both a gold mesh located on the beamline, and a Si photodiode located after the gas cell. In addition, an analog signal from a capacitance manometer was recorded simultaneously with the ion signal and incident photon flux to monitor target gas pressure for a point-by-point normalization of the recorded spectra. Due to this normalization and possible sensitivity differences in the detection of the fragments, the partial-ion yields are presented in this article in arbitrary units along a scale that is directly comparable for the different fragments. The working pressure in the target chamber was approximately 1×10^{-5} Torr, and the chamber was isolated from the beamline vacuum by differential pumping. Halocarbon 14, CF_4, was obtained commercially from Airgas, with a stated semiconductor grade purity of 99.999%, and introduced in the vacuum chamber without further purification.

III. RESULTS AND DISCUSSION

CF_4 is a closed-shell molecule belonging to the symmetry point group T_d. In an independent-particle approximation, its electronic structure is

$$\underbrace{(1a_1)^2(1t_2)^6}_{\text{F1}s}\ \underbrace{(2a_1)^2}_{\text{C1}s}\ \underbrace{(3a_1)^2(2t_2)^6}_{\text{inner valence}} \times \underbrace{(4a_1)^2(3t_2)^6(1e)^4(4t_2)^6(1t_1)^6(5t_2)^0(5a_1)^0}_{\text{outer valence}}.$$

where $(5t_2)^0$ and $(5a_1)^0$ are the lowest unoccupied molecular orbitals (LUMO). These two states consist of four degenerate antibonding orbitals formed from an admixture of the C sp^3 hybridized orbitals and F $2p$ orbitals [13]. We obtained total- and partial-ion yields for all detectable fragments in the photon-energy range 295–350 eV, including the C K edge at 301.80 eV, as well as the photon-energy range 680–750 eV, including the F K edge at 695.5 eV.

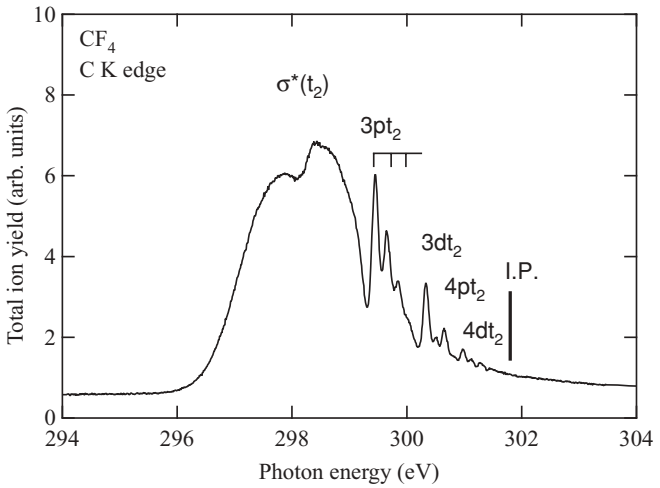

FIG. 1. Total-ion yield in the photon-energy region 294–306 eV including the C *K* edge at 301.8 eV. The spectral assignment and the energy calibration are taken from [20]. I.P. is the ionization threshold.

A. Carbon *K* edge

We show in Fig. 1 the total-ion yield (TIY), essentially equivalent to the absorption spectrum, in the photon-energy range 294–304 eV. The photon energy was calibrated on the $3pt_2$ Rydberg transition at 299.442 eV [20]. The literature assignment of the absorption spectrum is given by [20]. Although measurements were made up to 350 eV, the above-threshold region shows only a smooth continuum absent any notable structure. Therefore, we focus on the energy region below 304 eV.

The spectrum in Fig. 1 can be divided into two regions, the lower-photon-energy region includes two broad structures with maxima at 297.8 and 298.5 eV and a shoulder at ~299.5 eV, while the higher-photon-energy region includes a series of sharp peaks converging to the ionization threshold. The first region is assigned to transitions from the C 1*s* level to the lowest-lying molecular orbitals with antibonding character. Theoretical analysis of this spectral region has shown that to correctly describe the spectral shape, a vibronic model is necessary in which not only the Jahn-Teller coupling within the subspace of $\sigma^*(t_2)$ states but also the quasi-Jahn-Teller coupling between the $\sigma^*(a_1)$ and $\sigma^*(t_2)$ states must be taken into account. It was found in [13] that the C 1*s* electron can be excited to the a_1 state with the help of quasi-Jahn-Teller coupling, and this plays a crucial role in determining the structure of the main band. Therefore the observed structure corresponds to transitions to three overlapping states, two with a_1 and one with e symmetry. At higher energy, the series of sharp structures are assigned to Rydberg states (see [20] for detailed assignment).

The ionic fragments detected in the C *K*-edge region are six singly charged cations, CF_3^+, CF_2^+, CF^+, C^+, F^+, and F_2^+; five doubly charged cations, CF_3^{2+}, CF_2^{2+}, CF^{2+}, C^{2+}, and F^{2+}; and three anions, CF^-, C^-, and F^- (not included here).

The parent ion, CF_4^+, is not detected, in agreement with previous measurements [28], because the ground state of CF_4^+ is repulsive and fragments on a subpicosecond time scale by loss of a fluorine atom. This arises because the ground state of CF_4^+ lies above the thermodynamic dissociation energy to $CF_3^+ + F$. No triply charged ions were observed.

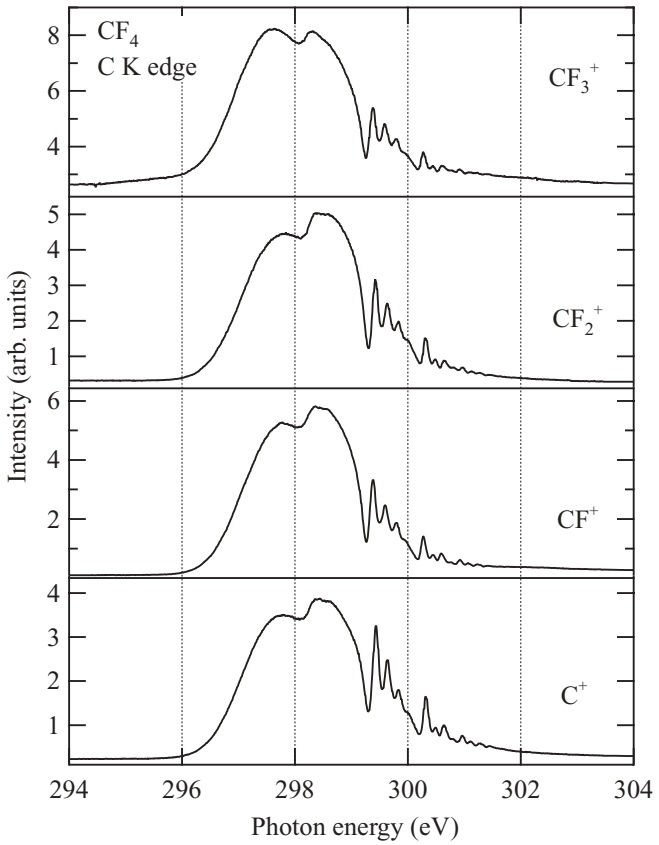

FIG. 2. Partial-ion yields for the cations CF_3^+, CF_2^+, CF^+, C^+ in the photon-energy region 294–304 eV around the C *K* edge.

We show in Fig. 2 the partial-ion yields obtained for the series CF_3^+, CF_2^+, CF^+, and C^+, which can be considered as the result of progressive fragmentation with subsequent loss of fluorine atoms. The main variation observed along this series is the change in relative intensity between the structures attributed to antibonding orbitals and the sharp structures related to Rydberg states. Following this scheme, the Rydberg series becomes more prominent. We have reported this effect for several other systems [23–25]. We attributed it to the fact that a core-to-Rydberg excited molecule is more likely to relax by spectator-Auger decay in which the excited electron is far from the nucleus, and then the system relaxes preferentially by emitting an electron from an orbital having strong overlap with the core hole, i.e., a valence orbital. In this scheme, the initially excited electron remains as a "spectator" and does not take part in the decay process. The resulting ion is still in an excited state and is more likely to dissociate as a consequence. We also observe that the intensity enhancement as a function of the extent of fragmentation involves all Rydberg excitations to the same extent, therefore we cannot identify any states with a significant Rydberg-valence mixing, as has been seen in other cases [23,29].

Another interesting experimental finding is that the broad structures at 297.8 and 298.5 eV, corresponding to transitions to the Jahn-Teller-split molecular orbitals, have the same relative intensity for all curves, with the exception of CF_3^+,

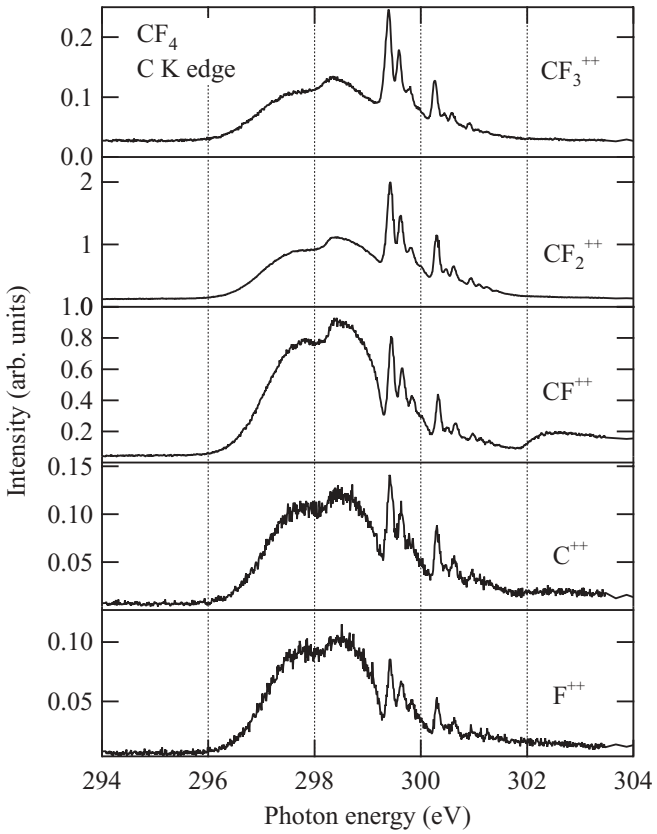

FIG. 3. Partial-ion yields for the doubly charged cations CF_3^{2+}, CF_2^{2+}, CF^{2+}, C^{2+}, and F^{2+} in the photon-energy region 294–304 eV around the C *K* edge.

where the lower-energy feature is more prominent. Similar effects are evident at the F *K* edge (see below). This difference is not due to different decay patterns after core excitation in the present case, because the resonant-Auger spectra are very similar at photon energies for the two main components of the broad structure [11,18]. Furthermore, the final state enhanced most is the $3t_2$ valence orbital, which should couple in a similar manner with the core-excited intermediate states. The most likely explanation is that the slightly higher energy absorbed by the system as a function of photon energy enhances the probability of subsequent fragmentation for the CF_3^+ fragment.

We show in Fig. 3 the partial-ion yields for all the doubly charged cations observed: CF_3^{2+}, CF_2^{2+}, CF^{2+}, C^{2+}, and F^{2+}. The C^{2+} and F^{2+} yields mimic those of their singly charged counterparts, suggesting these doubly charged species are produced by second-step Auger from the single ions. In contrast, the other doubly charged species (CF_3^{2+}, CF_2^{2+}, CF^{2+}) are produced by direct fragmentation, as evidenced by their differences with respect to the singly charged species. In the Rydberg region, the final states reached after spectator decay are unstable and fragment easily, therefore it is likely that fragmentation processes can lead directly to doubly charged fragments. Another factor is that such final states can be located above the double-ionization threshold. We note the ionization threshold is not visible in most of the cation yields, while it is usually quite pronounced, especially for doubly charged species (see, for example, [30]), because production of doubly charged cations should be enhanced by Auger decay above threshold. The fact that the edge is not clear in CF_4 can be attributed to the extended fragmentation into doubly charged species that is already possible in the below-threshold region. Resonant-Auger-decay experiments [11,18] have shown that the final states reached after excitation to the Jahn-Teller-split intermediate states are located at relatively high binding energy (i.e., resonant-Auger decay does not involve the lowest-lying final ionic states), therefore the decay reaches states with a relatively high energy content and/or states above the double-ionization threshold. As a result, the fragmentation patterns do not change substantially while crossing the ionization threshold. Such an observation has been reported in the literature [10]. The threshold is seen only in the CF^{2+} yield, with a typical onset due to post-collision interaction (PCI) recapture [30].

Another observation is that continuum structures that may be related to shape resonances or doubly excited states are barely or not visible in most of the cation yields. A shape resonance was reported for CF_4 in EELS [9] and photoionization cross-section measurements [26]. In our data, we see weak enhancement around 320 eV (not shown) in the total-ion yield and some of the cation yields, namely, C^{2+} and CF^{2+}. However, the effect is much less dramatic than in most of the other systems with a central atom surrounded by fluorine atoms (BF_3, SiF_4, SF_6), where shape resonances can be identified in the cation yields with much more spectral intensity (see, e.g., [31–33]). We note that in CF_4 one of the main characteristics of systems with a prominent potential barrier giving rise to shape resonances in the continuum, namely, the suppression of the Rydberg series, is not present. Apparently, the interplay between geometric and electronic structures which leads to potential-barrier effects is quite subtle.

B. Fluorine *K* edge

Figure 4 shows the total-ion-yield spectrum in the photon-energy range 680–715 eV. The energy calibration is based on the 692.9 eV position of the most intense below-threshold feature [20]. The main difference with respect to the C *K* edge is that the Rydberg series is suppressed. As before, the broad features below threshold are transitions to the antibonding $5t_2$ and $5a_1$ molecular orbitals. We observe three broad features at 691.2, 692.9, and 694.4 eV, which are assigned to transitions to antibonding a_1 and t_2 states. In analogy with the C *K* edge, these features are due to the Jahn-Teller splitting of the t_2 state and the quasi-Jahn-Teller mixing of the a_1 and t_2 states.

The same positive and negative fragments reported for the C *K* edge were observed at the F *K* edge, with the addition of triply charged F^{3+} (not shown). We measured all partial-ion yields up to 750 eV, but above threshold all of them show a smooth continuum, as seen above the C *K* edge. Therefore, we show only the photon-energy region 680–697 eV.

At the F *K* edge, the relative intensities of the spectral features related to Jahn-Teller and quasi-Jahn-Teller splitting vary significantly for different fragments, and we observe a strong state selectivity in the different fragmentation channels. Comparing partial yields along the series CF_3^+, CF_2^+, CF^+, C^+, and F^+, shown in Fig. 5, the lowest-lying feature at

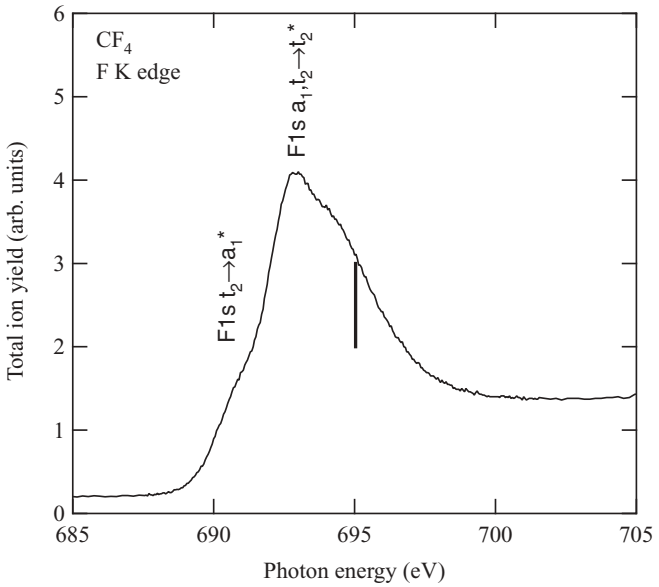

FIG. 4. Total-ion yield in the photon-energy region 685–705 eV, including the F *K* edge at 695.5 eV. The energy calibration and spectral assignment are in part taken from [19].

691.2 eV is prominent in CF_3^+ and CF^+, but not in CF_2^+ and C^+. The same strong state selectivity is observed in Fig. 6, where we show partial-ion yields for the doubly charged species CF_3^{2+}, CF_2^{2+}, CF^{2+}, C^{2+}, and F^{2+}. If we

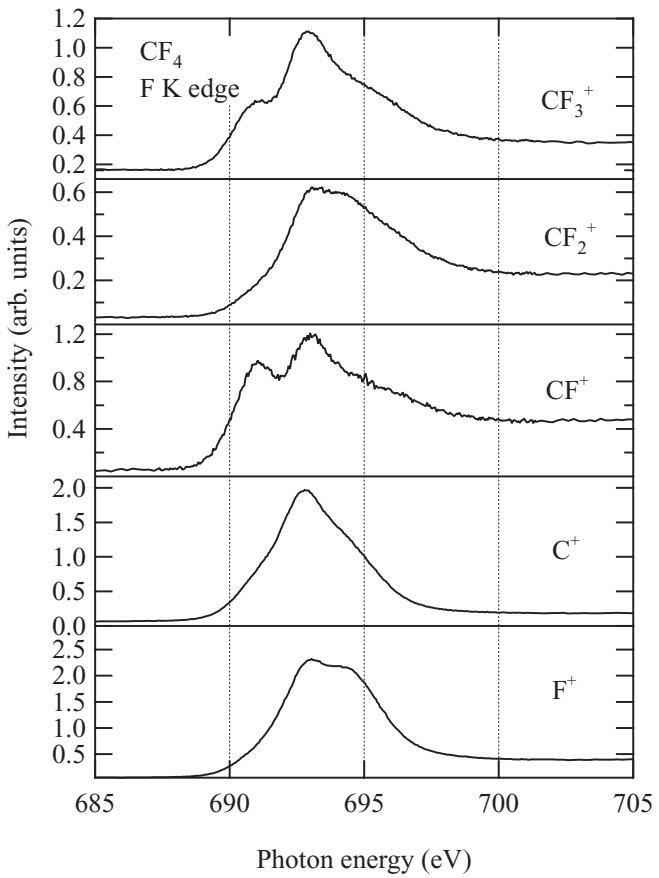

FIG. 5. Partial-ion yields for the cations CF_3^+, CF_2^+, CF^+, C^+, and F^+ in the photon-energy range 685–705 eV around the F *K* edge.

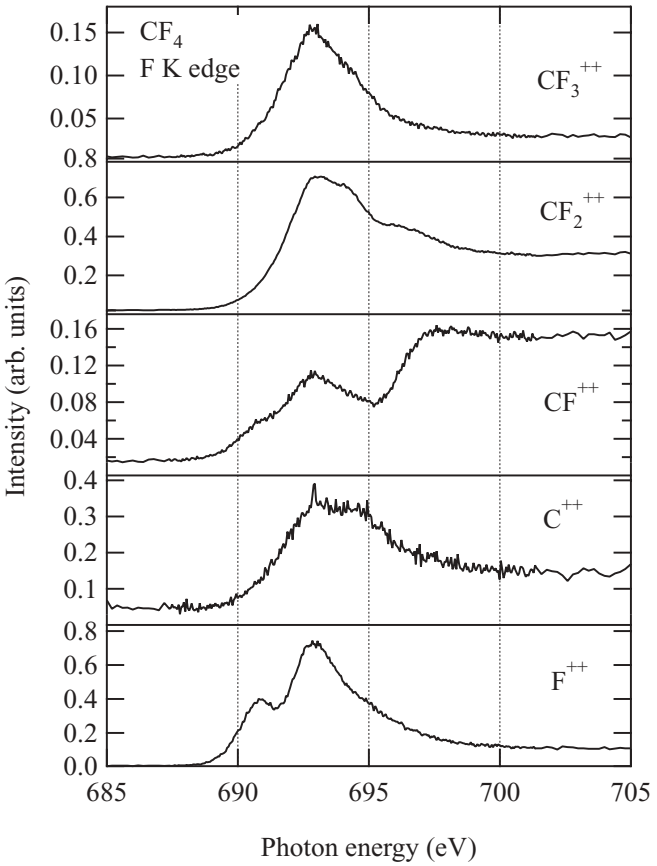

FIG. 6. Partial-ion yields for the doubly charged cations CF_3^{2+}, CF_2^{2+}, CF^{2+}, C^{2+}, and F^{2+} in the photon-energy range 685–705 eV around the F *K* edge.

compare the partial yields for F^+ (Fig. 5) and F^{2+} (Fig. 6), we observe that F^{2+} does not result from a second-step Auger decay from F^+, but must be produced by an entirely different decay channel, because of the prominence of the lowest-lying resonance and the depressed intensity on the higher resonance at 694.4 eV. This observation allows us to propose improved energy positions for the overlapping features: the lowest feature is at 691.04 eV instead of 691.2 eV as previously reported [20], and the highest-lying feature located at 694.7 eV [20] is more likely at 694.4 eV.

The main change in the partial-ion yields at the F *K* edge is the relative weight of the first and third spectral structures. According to the literature assignment, the peak at 691.04 eV should correspond to the F 1*s* $t_2 \rightarrow \sigma^* a_1$ transition, while the peak at 694.4 eV corresponds to a transition from the F 1*s* a_1 and t_2 states to the Jahn-Teller-split state of a_1 symmetry, although this is not specified in [20]. These two intermediate states are linked by the quasi-Jahn-Teller interaction. The detection of such different fragmentation patterns following the excitation to states with the same nature and molecular-orbital composition has no immediate explanation, although we can speculate about possible reasons. Symmetry breaking, anisotropic electron emission following resonant-Auger decay, and anisotropic F^+ ion emission have been reported for CF_4 at the F *K* edge [34,35]. In [35], the authors observed that the core-hole polarization can be transferred to the valence hole in the Auger-decay process. Antisymmetric nuclear motion,

due to vibronic coupling in the Auger final state, can then result in anisotropic ion fragmentation. In our data, this implies that in the photon-energy range of the A_1^* Jahn-Teller-split state, the final states undergo antisymmetric nuclear motion leading to anisotropic fragmentation. In [34], the authors observed Doppler splitting in the Auger emission of the atomiclike F* fragment, which they considered direct evidence that asymmetric nuclear motion proceeds in the F 1*s* excited state, preferentially along the direction of the polarization vector, leading to symmetry lowering from T_d to C_{3v}. The F $1s^{-1}a_1$ core-excited states consist of nearly degenerate A_1^* and T_2^* states. Coupling between the electron motion and the asymmetric nuclear motion causes pseudo-Jahn-Teller mixing between these A_1^* and T_2^* core-excited states, in addition to the Jahn-Teller mixing within T_2^*. When one C–F bond is elongated, the molecule changes to the C_{3v} point group, and the T_2^* state splits into A_1^* and E^* components. The A_1^* couples with the A_1^* state that originates in the symmetric CF_4 geometry. In our spectra, we clearly identify these three components. We observe that the fragments with more intensity at 691.04 eV are CF_3^+, CF^+, F^{2+} and F_2^+. The F^+ fragment appears to be more intense at the energy position of the E^* core-excited state. This discrepancy with the data in [34], in which F^+ is observed over the whole range of core-excited states, can be explained by the different time scales of the resonant-Auger and ion-yield experiments: in the electronic-decay time scale, ultrafast phenomena are observed, while in our experiment the ions travel for microseconds before reaching the spectrometer. Therefore, we only observe phenomena that take place in the final states reached after electronic decay rather than in the core-excited states.

Similar anisotropic fragmentation was observed following direct valence excitation to the unoccupied $5t_2$ and $5a_1$ orbitals in the 17–60 eV photon-energy range [36]. In this case, anisotropy in fragment emission was observed and interpreted on the grounds of preferential orientation of the molecular axis with respect to the polarization vector after symmetry lowering from T_d to C_{3v}: the dipole moment for the transition to the A_1 state is parallel to the C_{3v} axis, while it is perpendicular for a transition to the E state. In the case of core excitation, this implies the dissociation takes place preferentially along the C_{3v} axis following the F $1s \rightarrow a_1$ transition and perpendicular to the C_{3v} axis for the F $1s \rightarrow e$ transition. This would explain the fact that the fragments such as CF_3^+ and CF^+, detected with relatively higher intensity at the F $1s \rightarrow a_1$ transition, have the same symmetry as the CF_4^* distorted intermediate state, while fragments such as CF_2^+, enhanced at the F $1s \rightarrow e$ transition, do not.

IV. FORMATION OF F_2^+

Figure 7 compares the yields for the cations F^+ and F_2^+ at both edges. In both cases, we observe a small energy shift in the onset of formation of F_2^+ compared to F^+ and other ions. The low-energy side of the resonances, corresponding to excitation of low vibrational levels, is depressed in the F_2^+ yield. From the spectral differences observed, it is clear F_2^+ is not created only by recombination of two fluorine atoms after dissociation, but must also be formed by a direct process. Direct formation of F_2^+ requires intramolecular atomic rearrangement assisted by

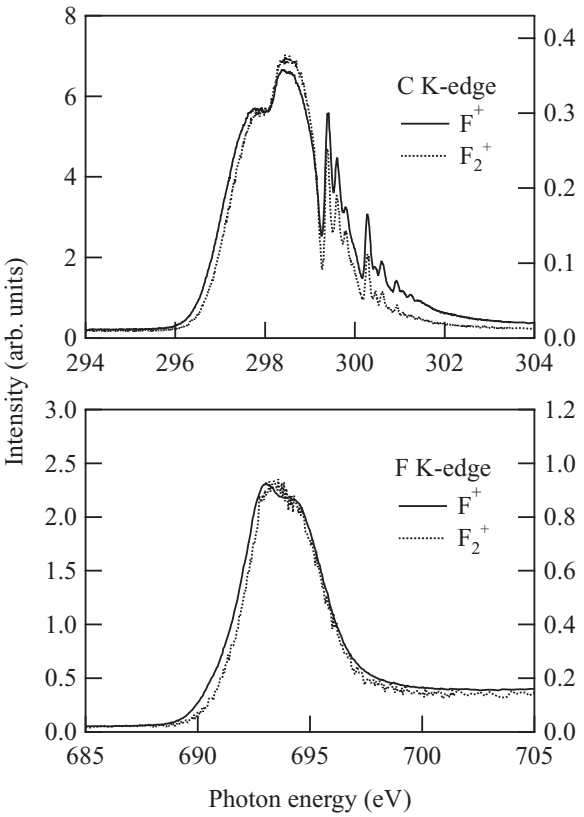

FIG. 7. Comparison of the partial-ion yields for the cations F^+ and F_2^+ at both edges: (top) the photon-energy region 294–304 eV around the C *K* edge; (bottom) the photon-energy range 685–705 eV around the F *K* edge.

vibrational excitation. Similar vibration-assisted intramolecular rearrangements involving light protons has been observed in the formation of H_2^+ from H_2O [37]; H_2^+, H_3^+, and HCl^+ from CH_3Cl [24]; and H_2^+, H_2O^+, and CH_2^+ from formic acid [29]. In the case of F_2^+, rearrangement naturally involves heavier atoms. We have reported similar cases of intramolecular rearrangement, such as formation of O_2^+ after C 1*s* core excitation in formic acid [29], and N_2^+ after C 1*s* core excitation in cyanogen [38]. Formation of F_2^+ was also found after F 1*s* core excitation in BF_3 [33]. In all these cases, it was found that excitation of high vibrational levels in bending modes was crucial. In the present case, the well-known deformation from T_d to C_{3v} symmetry through fast nuclear motion in the core-excited state brings the F atoms closer together and probably assists in the formation of F_2^+.

V. CONCLUSION

By means of partial-ion-yield spectroscopy, we have observed strong differences in the fragmentation pathways after core excitation in CF_4 at both the carbon and fluorine *K* edges. The partial-ion yields all reveal spectral features related to Jahn-Teller and quasi-Jahn-Teller splitting. Although all ion yields show these features at both edges, the partial-ion yields obtained for the series CF_3^+, CF_2^+, CF^+, C^+, and F^+ at the F *K* edge provided an opportunity to observe the influence of symmetry on molecular fragmentation, since the production of CF_2^+, C^+, and F^+ is almost completely turned off on the

F $1s \rightarrow a_1$ resonance. Without further theoretical calculations, we can only speculate that the system undergoes fragmentation following different pathways depending on the symmetric or antisymmetric nuclear motion initiated by the excitation to core-excited states with potential-energy surfaces that differ strongly at out-of-equilibrium geometries as described in [18]. Multidimensional calculations of the core-excited potential-energy surfaces would be necessary to further interpret the observations. Finally, direct formation of the F_2^+ fragment through excitation of high vibrational levels is observed and discussed on the grounds of molecular deformation from T_d to C_{3v} symmetry due to strong Jahn-Teller coupling.

ACKNOWLEDGMENTS

The authors thank the staff of the ALS for their excellent support. Support from the National Science Foundation under NSF Grant No. PHY-05-55699 is gratefully acknowledged. This work was performed at the Advanced Light Source, which is supported by DOE (DE-AC03-76SF00098).

[1] A. P. Hitchcock, M. Pocock, and C. E. Brion, Chem. Phys. Lett. **49**, 125 (1977).
[2] G. C. King and F. H. Read, J. Phys. B **12**, 137 (1979).
[3] M. Tronc, G. C. King, R. C. Bradford, and F. H. Read, J. Phys. B. **9**, L555 (1976).
[4] W. Zhang, T. Ibuki, and C. E. Brion, Chem. Phys. **160**, 435 (1992).
[5] J. Schirmer, A. B. Trofimov, K. J. Randall, J. Feldhaus, A. M. Bradshaw, Y. Ma, C. T. Chen, and F. Sette, Phys. Rev. A **47**, 1136 (1993).
[6] G. Remmers, M. Domke, and G. Kaindl, Phys. Rev. A **47**, 3085 (1993).
[7] A. Koch and S. D. Peyerimhoff, Chem. Phys. Lett. **195**, 104 (1992).
[8] K. Ueda, M. Okunishi, H. Chiba, Y. Shimizu, K. Ohmori, Y. Sato, E. Shigemasa, and N. Kosugi, Chem. Phys. Lett. **236**, 311 (1995).
[9] G. R. Wight and C. E. Brion, J. Electron Spectrosc. Relat. Phenom. **4**, 327 (1974).
[10] D. A. Lapiano-Smith, C. I. Ma, K. T. Wu, and D. M. Hanson, J. Chem. Phys. **90**, 2162 (1989).
[11] M. Neeb, A. Kivimäki, B. Kempgens, H. M. Köppe, and A. M. Bradshaw, J. Phys. B **30**, 93 (1997).
[12] B. S. Itchkawitz, B. Kempgens, H. M. Köppe, J. Feldhaus, A. M. Bradshaw, and W. B. Peatman, Rev. Sci. Instrum. **66**, 1531 (1995).
[13] S. I. Itoh, S. Tanaka, and Y. Kayanuma, Phys. Rev. A **60**, 4488 (1999).
[14] J. A. Stephens, D. Dill, and J. L. Dehmer, J. Chem. Phys. **84**, 3638 (1986).
[15] J. A. Tossell and J. W. Davenport, J. Chem. Phys. **80**, 813 (1984).
[16] K. Ueda, Y. Shimizu, H. Chiba, M. Okunishi, K. Ohmori, Y. Sato, E. Shigemasa, and N. Kosugi, J. Electron Spectrosc. Relat. Phenom. **79**, 441 (1996).
[17] M. K. Thomas, B. O. Fisher, P. A. Hatherly, K. Codling, M. Stankiewicz, and M. I. Roper, J. Phys. B **32**, 2611 (1999).
[18] K. Ueda, M. Simon, C. Miron, N. Leclercq, R. Guillemin, P. Morin, and S. Tanaka, Phys. Rev. Lett. **83**, 3800 (1999).
[19] N. Saito, J. D. Bozek, and I. H. Suzuki, Chem. Phys. **188**, 367 (1994).
[20] M. de Simone, M. Coreno, M. Alagia, R. Richter, and K. C. Prince, J. Phys. B **35**, 61 (2002).
[21] J. Kikuma and B. P. Tonner, J. Electron Spectrosc. Relat. Phenom. **82**, 41 (1996).
[22] S.-Y. Chen, C. I. Ma, D. M. Hanson, K. Lee, and D. Y. Kim, J. Electron Spectrosc. Relat. Phenom. **93**, 61 (1998).
[23] M. N. Piancastelli, W. C. Stolte, G. Öhrwall, S.-W. Yu, D. Bull, K. Lantz, A. S. Schlachter, and D. W. Lindle, J. Chem. Phys. **117**, 8264 (2002).
[24] D. Céolin, M. N. Piancastelli, R. Guillemin, W. C. Stolte, S.-W. Yu, O. Hemmers, and D. W. Lindle, J. Chem. Phys. **126**, 084309 (2007).
[25] D. Céolin, M. N. Piancastelli, W. C. Stolte, and D. W. Lindle, J. Chem. Phys. **131**, 244301 (2009).
[26] C. M. Truesdale, D. W. Lindle, P. H. Kobrin, U. E. Becker, H. G. Kerkhoff, P. A. Heimann, T. A. Ferrett, and D. A. Shirley, J. Chem. Phys. **80**, 2319 (1984).
[27] W. C. Stolte, R. Guillemin, S.-W. Yu, and D. W. Lindle, J. Phys. B **41**, 145102 (2008).
[28] J. C. Creasey, H. M. Jones, D. M. Smith, R. P. Tuckett, P. A. Hatherly, K. Codling, and I. Powis, Chem. Phys. **174**, 441 (1993).
[29] R. Guillemin, W. C. Stolte, and D. W. Lindle, J. Phys. B **42**, 125101 (2009).
[30] R. Guillemin, W. C. Stolte, L. T. N. Dang, S.-W. Yu, and D. W. Lindle, J. Chem. Phys. **122**, 094318 (2005).
[31] M. N. Piancastelli, W. C. Stolte, R. Guillemin, A. Wolska, and D. W. Lindle, J. Chem. Phys. **128**, 134309 (2008).
[32] M. N. Piancastelli, W. C. Stolte, R. Guillemin, A. Wolska, S.-W. Yu, M. M. Sant'Anna, and D. W. Lindle, J. Chem. Phys. **122**, 094312 (2005).
[33] R. Guillemin *et al.* (to be published).
[34] Y. Muramatsu, K. Ueda, Y. Shimizu, H. Chiba, K. Amano, Y. Sato, and H. Nakamatsu, J. Phys. B **32**, L213 (1999).
[35] K. Ueda *et al.*, Phys. Rev. Lett. **90**, 233006 (2003).
[36] Y. Hikosaka and E. Shigemasa, J. Electron Spectrosc. Relat. Phenom. **152**, 29 (2006).
[37] M. N. Piancastelli, A. Hempelmann, F. Heiser, O. Gessner, A. Rüdel, and U. Becker, Phys. Rev. A **59**, 300 (1999).
[38] G. Öhrwall, W. C. Stolte, R. Guillemin, S.-W. Yu, and D. W. Lindle, J. Phys. B **43**, 095201 (2010).